Modelling of the over-exposed pixel area of CCD cameras caused by laser dazzling

Koen W. Benoist, Ric (H.)M.A. Schleijpen
TNO, Oude Waalsdorperweg 63, 2597 AK, The Hague, The Netherlands

ABSTRACT

A simple model has been developed and implemented in Matlab code, predicting the over-exposed pixel area of cameras caused by laser dazzling. Inputs of this model are the laser irradiance on the front optics of the camera, the Point Spread Function (PSF) of the used optics, the integration time of the camera, and camera sensor specifications like pixel size, quantum efficiency and full well capacity. Effects of the read-out circuit of the camera are not incorporated. The model was evaluated with laser dazzle experiments on CCD cameras using a 532 nm CW laser dazzler and shows good agreement. For relatively low laser irradiance the model predicts the over-exposed laser spot area quite accurately and shows the cube root dependency of spot diameter on laser irradiance, caused by the PSF as demonstrated before for IR cameras. For higher laser power levels the laser induced spot diameter increases more rapidly than predicted, which probably can be attributed to scatter effects in the camera. Some first attempts to model scatter contributions, using a simple scatter power function f(θ), show good resemblance with experiments. Using this model, a tool is available which can assess the performance of observation sensor systems while being subjected to laser countermeasures.

Keywords: Laser-dazzling, imaging system, CCD-camera

1. INTRODUCTION

Laser dazzling can be used as an optical countermeasure against cameras to prevent the operator to perform his task, for instance a military operator of CLOS (Command to Line Of Sight) weapons. By using lasers one can deny the weapon operator to fulfill his task being acquisition, tracking and designation of a target. The distance between CLOS operator and target in general is relatively large (order kilometers) so small camera FOVs will be used then. The effect of laser irradiance on infrared camera systems has been explored and reported before, however little is published about the effects of lasers on visible cameras like CCD or CMOS cameras.

Experiments on infrared cameras (references 1, 2) have shown that, for relatively low dazzling laser power levels, the size of the induced over-exposed pixel area on CCD camera sensors can be explained by the Point Spread Function (PSF) of the optics of the camera. The dependence of the diameter of this area can be described as a function of the cube root of the laser irradiance. For higher power levels the dazzling area starts to grow faster, which is attributed to the scatter effects in the camera.

Durécu et al. (reference 3) reported on laser dazzling effects on TV-cameras using a pulsed laser under different dazzling conditions. Laser dazzling effects that were observed were pixel saturation, increasing over-exposed area of pixels with increasing pulse energy, lens effects like reflections, diffractions and scattering, and electronic effects like pixel column saturation (blooming). No detailed quantitative analysis was carried out on the results. In reference 5, Zhen Zhang et al. describe dazzling effects on scanning linear array CCD cameras using a 1064 nm CW laser. They reported on the appearance of two sideward spots besides the main laser spot and attributed this to multiple reflections between lens and CCD camera.

In this paper experiments on the effects of CW laser irradiance on visible CCD cameras are described. Experiments were carried out on a number of visible band CCD cameras which were subjected to defined levels of laser irradiance at 532 nm, as described in section 2 of this paper. A simple model has been developed to predict the size of the over-exposed pixel area of cameras caused by laser dazzling. This model is described in section 3 and model predictions are compared with experimental results in section 4. In section 5 a modification to the model is proposed to incorporate scatter contribution, which were observed in the experimental results. Finally conclusions are drawn in section 6.

*koen.benoist@tno.nl; phone +31 88 866 40 88; www.tno.nl

Technologies for Optical Countermeasures XI; and High-Power Lasers 2014: Technology and Systems, edited by David H. Titterton, Mark A. Richardson, Robert J. Grasso, Willy L. Bohn, Harro Ackermann, Proc. of SPIE Vol. 9251, 92510H · © 2014 SPIE · CCC code: 0277-786X/14/$18 · doi: 10.1117/12.2066305

2. LASER DAZZLE EXPERIMENTS

To investigate the phenomena appearing while visual cameras are subjected to laser irradiance of different levels laser dazzle experiments are carried out with the set-up schematically shown in Figure 1. A 532 nm CW laser (CNI Type MGL532) with a maximum laser power of 400 mW was used to perform the experiments. The laser power was varied by changing the laser current and using neutral density filters. The laser beam was directed on the lens of the camera using beam expanders to completely fill the aperture of the camera. Three different branches of CCD cameras were used, two monochrome CCD cameras (Philips LDH 0703 and Sony AVC-D5CE) and one color camera (Sony XC-777). An identical lens (f=25 mm, f/1.4) was mounted on all cameras during the experiments, and automatic functions of the cameras like AGC (Automatic Gain Control) etc. were disabled. The integration time of the cameras was set around 20 msec.

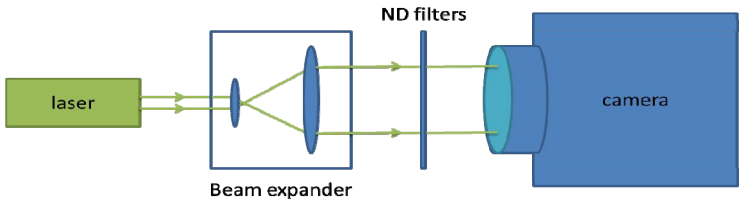

Figure 1 Schematic overview of the laser dazzling set-up

The behavior of the camera was monitored while increasing the laser output power, until no change in effects was observed any more. The output power of the laser was measured using a Liconix Model 45PM power meter. Digitized images of the cameras were recorded during the dazzling experiments as well as digitized oscilloscope images of camera video lines. Depending on the laser irradiance level typically the following phenomena were observed, see Figure 2:

- A growing area of over-exposed and saturated pixels (laser induced over-exposed spot) with increasing laser irradiance level
- Blooming effect (saturated vertical lines) which is characteristic for CCD cameras when exposed by high intensity light sources
- Unstable video output at high irradiance levels (>10^8 pW/cm^2)
- A (reversible) break-down of the video output at higher irradiance levels, resulting in completely black images

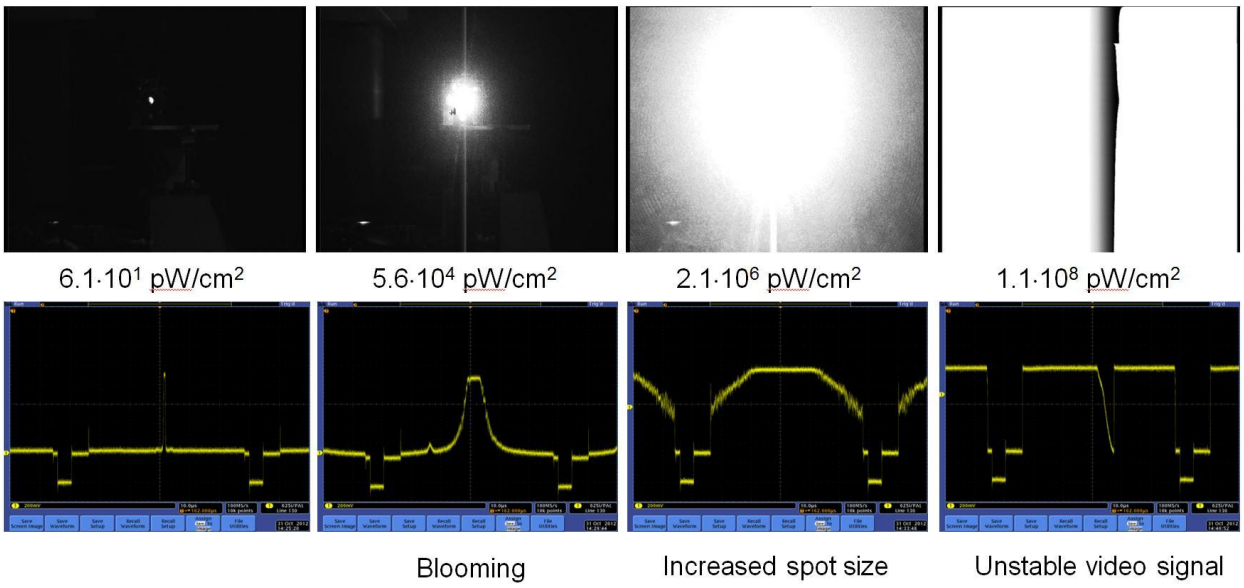

Figure 2 Typical observed laser dazzling effects on the Philips CCD camera for different laser irradiance levels. Shown are digitized camera images (upper part) and corresponding oscilloscope images of camera video lines

From the recorded camera images the total number of over-exposed pixels, within the laser induced spot area, was determined as a function of laser irradiance level, and a laser induced spot diameter was calculated assuming a circular over-exposed spot area. In Figure 3 this laser induced spot diameter is plotted as a function of laser irradiance level (in pW/cm^2) for the three different cameras.

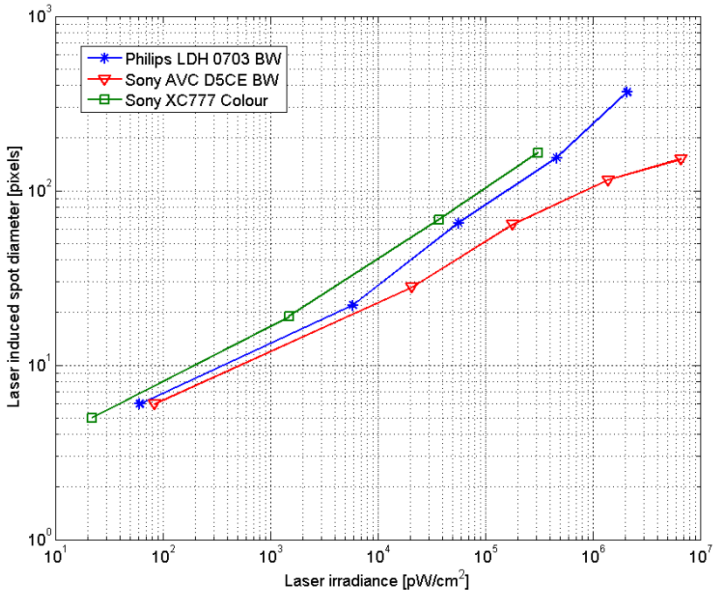

Figure 3 Diameter of the laser induced over-exposed area as a function of laser irradiance for different CCD cameras

As can be seen from the figure all cameras show more or less a cube root dependency on laser irradiance, which is in agreement with what is found for IR camera dazzling and reported in reference 1. In that paper it was shown that this result can be explained by an expression derived from the point spread function (PSF) of the optics in front of the camera, and was independent of the read-out mechanism of the camera.

Because it turns out that only the optics is involved in the determination of the size of the laser induced over-exposed spot area for CCD cameras, it was decided to develop a model based on the PSF of the camera optics to be able to predict the size of the over exposed pixels area as a function of laser irradiance and camera integration time. The only input parameters are the camera specifications which determine the number of electrons which are generated in the detector array elements: quantum efficiency, detector fill factor and pixel full well capacity. This model is described in the following section.

3. LASER INDUCED OVER-EXPOSED PIXEL AREA

The minimum spot size or resolution of optical lenses is given by the Point Spread Function or PSF, which is the Fourier Transform of the MTF (Modulation Transfer Function). The formula of the diffraction limited MTF (DTF) of a lens is given by

$$\mathrm{DTF} = \frac{2}{\pi} \cdot \left(\cos^{-1}(\nu) - \nu \cdot \sqrt{1-\nu^2} \right) \qquad [1]$$

With ν the normalized spatial frequency given by f/f_{cut} where f is the spatial frequency and f_{cut} is the cut-off frequency equal to $D/f\lambda$, with D the lens aperture, f the focal length and λ the wavelength. The theoretical PSF of a circular aperture is the so called Airy function. The shape of the Airy function is only dependent on the F-number $F\# = f/D$ of the lens and the wavelength λ. This Airy function has, besides a high central peak, side lobes whose intensity decreases rapidly from the center, see Figure 4.

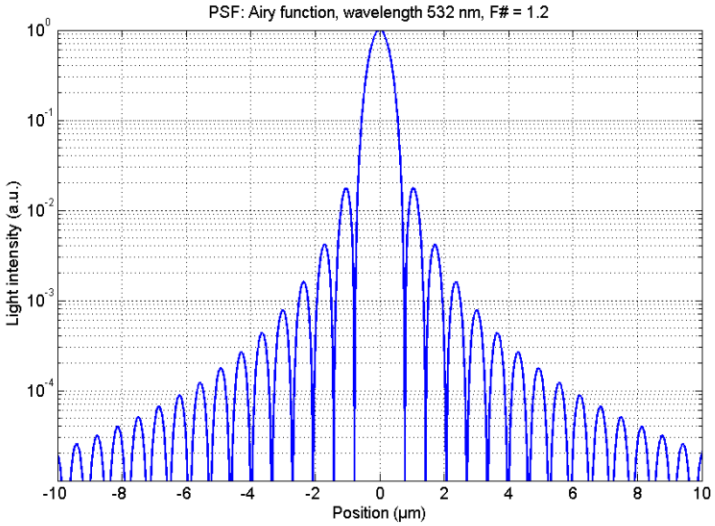

Figure 4 Logarithmic plot of the diffraction limited PSF of a lens with f#=1.2 (λ=532 nm)

For normal camera use these side lobes will play a minor role, but they can become important when high light intensities are involved like in the case of laser dazzling. Collimated laser light illuminating a CCD camera lens, which is focused at infinity, will be projected on the CCD array with a light distribution given by the PSF of the lens. So the size of the area of over-exposed pixels of a CCD camera, caused by a laser dazzler producing a laser irradiance E [W/m^2] at the front optics, in principle can be calculated when the PSF and transmission of the camera lens are known, as well as the characteristics of the CCD array of the camera. The diffraction limited PSF of the optics is determined by the focal length f and aperture D of the lens. The relevant CCD characteristics are pixel size and fill factor, frame integration time T_{int} of the camera, quantum efficiency QE and full well capacity of the CCD sensor array pixels.

Collimated laser light impinging on the front optics will be imaged onto the CCD array with a light flux Φ [W] given by:

$$\Phi(x,y) = \Phi_{CCD} \cdot PSF(x,y) \qquad [2]$$

With PSF(x,y) the normalized 2D-Airy function in case of a circular aperture and the total light flux Φ_{CCD} falling on the CCD sensor array which is given by:

$$\Phi_{CCD} = \pi \cdot \frac{D^2}{4} \cdot E \cdot \tau_{opt} \qquad [3]$$

Where D is the lens aperture, and τ_{opt} the transmission of the lens. Laser irradiance is assumed constant over the lens here. The light energy Q [J] accumulated by a CCD pixel element is determined by the integrated received light flux over the area A_{pix} of the specified pixel, taking into account the pixel fill factor, and the integration time of the camera T_{int}:

$$Q_{pix} = T_{int} \cdot \iint_{A_{pix}} \Phi(x,y)\,dx\,dy = \pi \cdot \frac{D^2}{4} \cdot E \cdot \tau_{opt} \cdot T_{int} \cdot \iint_{A_{pix}} PSF(x,y)\,dx\,dy \qquad [4]$$

The number of photons falling on the pixel is equal to this energy Q_{pix} divided by the single photon energy. The number of electrons generated in the pixel is then determined by the quantum efficiency QE of the sensor at the specified laser wavelength λ. The maximum number of electrons that can be stored in a single pixel is given by the full well capacity of the sensor, the amount of charge an individual pixel can hold before saturating. So given the laser irradiance and the camera integration time, equation [4] can be used to determine the spot distribution induced by a laser over the CCD array and subsequently the area of laser induced over-exposed pixels.

In this model the calculated saturated spot area is completely determined by the optics of the camera and the optoelectronic specifications of the sensor array itself, and is independent of sensor read-out and electronics which are present in the camera. This means that this model can be used to predict laser dazzle over-exposed spot areas for different types of camera and for different camera settings like integration time and diaphragm.

To verify model predictions of saturated pixel areas with experiments, a Matlab script is written to calculate the number of collected electrons in the pixels of a 2D-CCD array based on the formulas given above. First for a given CCD camera sensor with specified optics, the Fourier transform of the 2D-DTF is calculated to obtain the 2D-PSF of the optics. Then, using formula [4], the accumulated laser energy per pixel is calculated by integrating the light intensity for every pixel of the 2D-array, and subsequently the number of electrons produced in every pixel is determined. The laser energy density (J/m^2) is obtained by multiplying the laser irradiance at the lens with the camera integration time. Subsequently, as a function of laser irradiance, camera integration time the total number of saturated pixels can be obtained, taking into account the full well capacity.

In real practice, camera lenses are not diffraction limited, and will be subjected to aberrations. To account for this effect in the model, we used the aberration transfer function as proposed by Shannon (reference 5). As was shown, the MTF-curve of a lens can be approximated as a product of the diffraction-limited DTF and an aberration transfer function (ATF), which is based upon the magnitude of the wavefront error, and an empirical constant 0.18:

$$\mathrm{ATF} = 1 - \left(\frac{W_{\mathrm{rms}}}{0.18}\right)^2 \cdot (1 - 4 \cdot (\nu - 0.5)^2) \qquad [5]$$

In this equation W_{rms} is the root-mean-square (rms) wavefront error expressed as fraction of waves. The rms wavefront error is related to the peak-to-peak wavefront error by $W_{rms} = W_{pp}/3.5$ (reference 6). $W_{pp} = 0.25$ simulates the wavefront error that typically occurs during manufacturing. Equation [5] is valid for small wavefront errors ($W_{pp}<0.5$), which is a reasonable limit for well-designed optics. For an illustration of the impact of aberration, Figure 5 (left) shows the MTF of an aberrated optical lens system for different wavefront errors. The corresponding normalized PSFs for f#=1.2, calculated by taking the Fourier transform of the MTF, are given in the right plot of Figure 5. As expected, the PSF gets broader with increasing aberration.

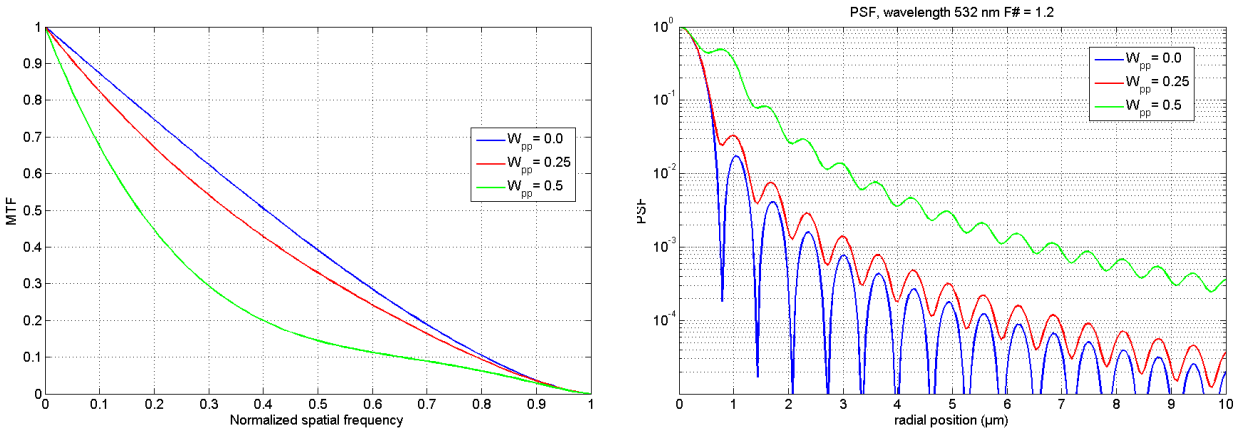

Figure 5 MTF (left) and PSF (right) of an aberrated optical lens system (F#=1.2) for different wavefront errors

4. MODEL VALIDATION

To verify the model described in section 3 of this paper, laser dazzle experiments with the same set-up as described before (see section 2 and Figure 1) were carried out. This time we used a camera having detailed sensor specifications, being an AVT Marlin F-033B fire-wire CCD camera, equipped with a Sony ICX414 CCD-sensor having a resolution of 656 x 494 pixels, a pixel pitch of 9.9 µm, a QE of approximately 38% at 532 nm (including fill factor), and a specified full well capacity of 32000 electrons. The integration time of the camera could be adjusted remotely between 32 µs and 67 seconds. The focal length of the camera was 75 mm and the lens, having an F-number of 4, was focused at infinity during the experiments.

In a first experiment, the effects on the camera subjected to laser dazzle was monitored while increasing the laser output power at a fixed camera integration time of 20 msec. Digitized images of the cameras were captured during the dazzling experiments, see Figure 6, and afterwards the total number of overexposed pixels N was determined. Here the overexposed pixels caused by blooming effects (vertical column of saturated pixels) were discarded. The laser induced spot diameter of the overexposed pixel area is then calculated by $D = 2*(N/\pi)^{1/2}$. For the AVT Marlin camera this means that the maximum diameter will be given by $D = 2*(656*494/\pi)^{1/2} = 642$ pixels.

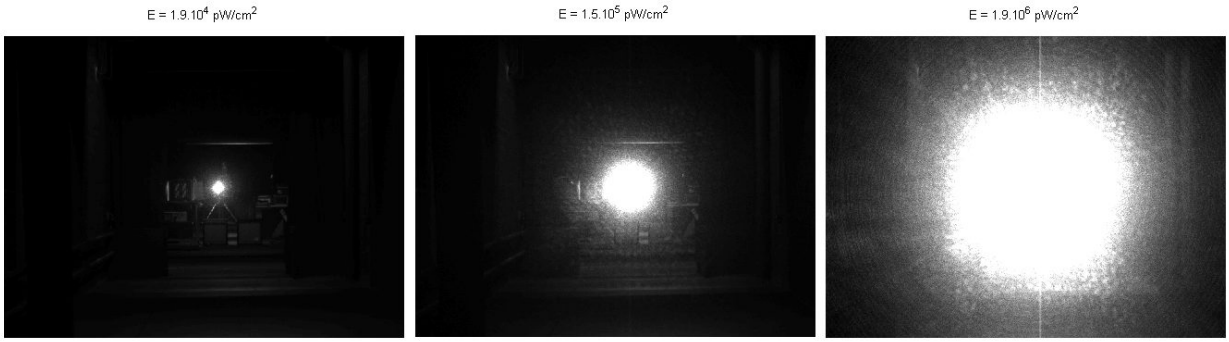

Figure 6 Images of the AVT Marlin CCD showing laser induced spots for different laser irradiance levels

To fit the model predictions to the experimental values an rms wavefront error of W_{rms}=0.14 was used. The experimental results of laser induced over-exposed spot diameter versus laser irradiance level are given in Figure 7, together with a model simulation using the camera parameters mentioned above (straight red line), a model simulation without lens aberration (red dashed line, W_{pp}=0), and a fit of a cube root dependency on laser irradiance (black dotted line). The model predictions in this double logarithmic plot show a discrete increment in laser induced over-exposed spot diameter at low irradiance levels. This is caused by the discretization in the number of over-exposed pixel N, leading to discrete steps in the laser induced over-exposed spot diameter D.

As can be seen, for a laser irradiance below $2 \cdot 10^4$ pW/cm^2 the experimental values match the model predictions accurately for W_{pp}=0.14. Both experimental and model simulation results, both with and without aberration, show the cube root dependency of spot diameter on the laser irradiance. For higher laser irradiance, the calculated diameter of the induced laser spot from the experimental results increases more rapid than predicted by the model. This effect has been observed before (reference 1), and probably can be attributed to scatter effects for instance from the camera lens.

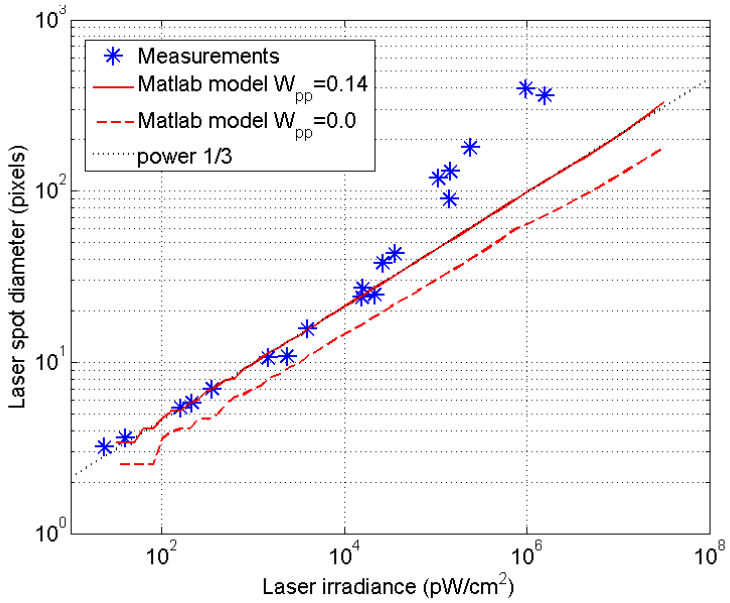

Figure 7 Laser induced over-exposed spot diameter as a function of laser irradiance

In a second experiment, the integration time of the AVT Marlin camera was changed for different fixed laser irradiance values. This because it is easier to change the integration time at fixed irradiance levels, than to change the laser irradiance by varying laser current and using ND-filters, because in the latter case the laser irradiance has to be measured for every measurement point. In this experiment a lens with a focal length of 75 mm and an F-number of 1.2 focused at infinity was used. Results are given in Figure 8 for laser induced over-exposed spot diameter versus camera integration

time for four laser irradiance levels. In Figure 9 the spot diameter is plotted against laser energy density, which is obtained by multiplying laser irradiance with camera integration time for every experimental point of Figure 8. From Figure 9 it can be seen that the results for the 4 used laser irradiance levels nicely overlap, as would be expected.

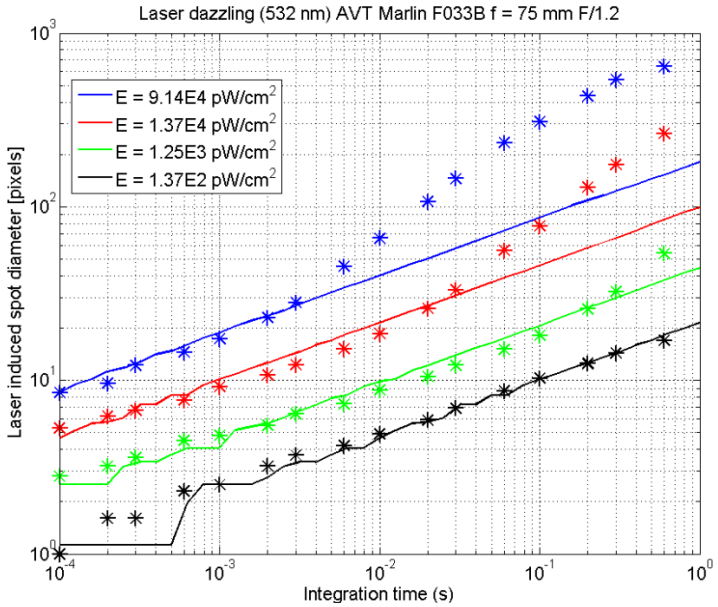

Figure 8 Experimental (*) and modelling results (lines) of the laser induced over-exposed spot diameter vs camera integration time

As before a good correspondence between experimental values and model for low laser irradiance levels is seen, using the same camera parameters as before. For very low energy densities (<1 nJ/m^2) the experimental results seem to deviate, but one should bear in mind that the spot diameter in this regime is only 1 or 2 pixels. For laser energy densities higher than approximately 3 µJ/m^2 the induced over-exposed spot diameter starts to increase more rapidly than predicted by the model. At the highest laser energy density that is used it can be seen that the complete CCD array starts to saturate; the laser induced spot diameter converges towards the maximum of 642 pixels.

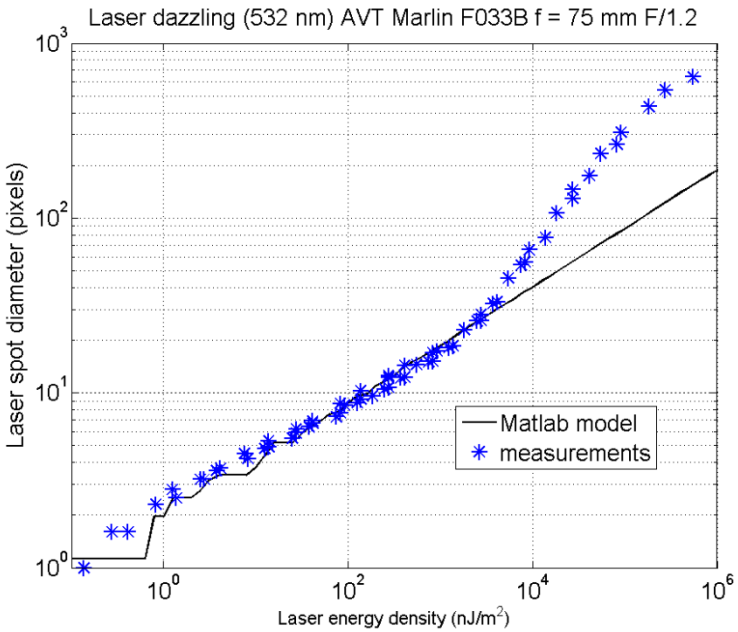

Figure 9 Experimental and modelling results of the laser induced over-exposed spot diameter vs laser energy density at lens

From the experiments it is concluded that the model developed for predicting the saturated area of overexposed pixels is accurate at low laser energy density values. At higher levels the saturated area grows faster, probably caused by contributions like internal (multiple) reflections and scattering. To account for scatter contributions at these higher energy levels, an attempt to incorporate scatter effects in the model has been carried out. This modified model is explained and verified in the next section.

5. SCATTER CONTRIBUTION MODELLING

Scattering effects may be facilitated by light which is scattered from different parts of the imaging sensor, but may also be due to e.g. lens imperfections, lens flares and/or dust particles. The amount of scattered light may vary considerably with entrance angle depending on the quality of the material. Also scattering from components such as housing and dome edges forms an additional unpredictable factor. Therefore it is nearly impossible to estimate reliably to what extent light is scattered by an optical setup such as a camera.

To incorporate scatter effects in our model we therefore used a scatter function f(θ) consisting of a power function with a constant factor a and an exponent b: $f(\theta) = a \cdot \theta^b$. This kind of scatter function is used for instance to describe scattering effects on windscreens (reference 7). The scatter function of course will be very dependent on the lens used, and for each lens different coefficients a and b are expected resulting from the way light is scattered in the lens.

The scatter function f(θ) is superimposed over the light intensity distribution as created by the PSF of the camera lens as described in section 3 of this paper. We used the data of the laser dazzle experiments of Figure 8 and changed coefficient a and b such to obtain a good match between modeling results and the experimental values at different laser power levels. For the used lens the fit values of $a = 4.2 \cdot 10^{-12}$ and b = -1.1 were found, see Figure 10. As can be seen a reasonable fit between experimental results and model can be obtained.

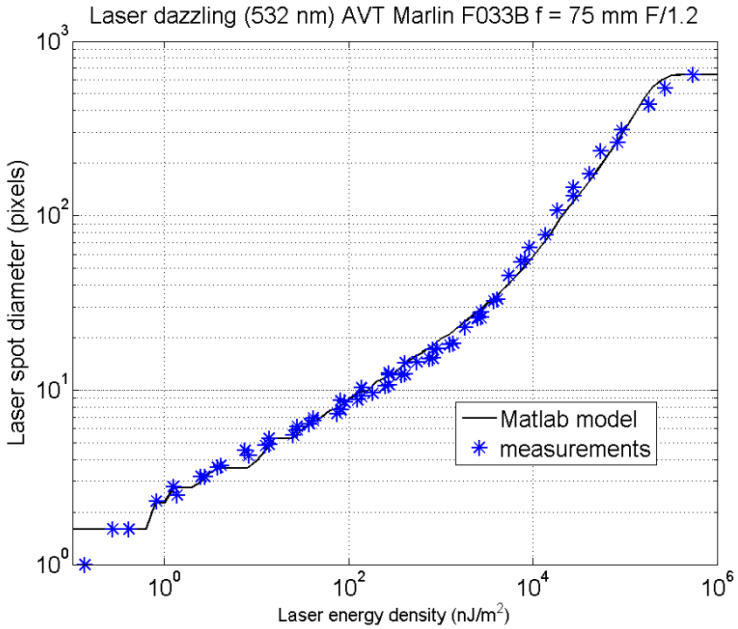

Figure 10 Comparison of model including scatter function with experimental results

Although good results have been obtained using a fitted scatter function as described above, the physical background cannot be understood from this function. In the future we will look for a better theoretical understanding of this scatter contribution.

6. CONCLUSIONS

In this paper we have described a model predicting the over-exposed pixel area of a CCD camera when subjected to CW laser irradiance. The model is based on optical effects only and does not take into account effects from the electronic

read-out. Experimental validation of the model shows that for low energy densities the model accurately predicts the area of over-exposed pixels. At higher energy levels scatter contributions cause a mismatch between experimental results and model predictions. In the model this is accounted for by incorporating a simple scatter function using two parameters, which can be fitted to the experimental results for the camera lens in use. Using this model, a tool is available which can assess the performance of visible camera sensor systems while being subjected to laser radiation.

REFERENCES

[1] H.M.A. Schleijpen, J.C. van den Heuvel, A.L. Mieremet, B. Mellier, F.J.M. van Putten, 'Laser Dazzling of Focal Plane Array Cameras', SPIE Vol. 6543: Infrared Imaging Systems: Design, Analysis, Modeling, and Testing XVIII, Orlando, April 2007

[2] H.M.A. Schleijpen, A. Dimmeler, B. Eberle, J.C. van den Heuvel, A.L. Mieremet, H. Bekman, B. Mellier, 'Laser Dazzling of Focal PLane Array Cameras', SPIE Vol. 6738: Technologies for Optical Countermeasures IV, Florence, September 2007

[3] A. Durécu, P. Bourdon, D. Fleury, O. Vasseur, 'Laser-dazzling effects on TV-cameras : analysis of dazzling effects and experimental parameters weight assessment', SPIE Vol. 6738: Technologies for Optical Countermeasures IV, Florence, September 2007

[4] Zhen Zhang, Xiang-ai Cheng, Tian Jiang, Zong-fu Jiang, 'A dazzling phenomenon of CW laser on linear CCD camera', Optik 123, p. 223– 227, 2012

[5] R.R. Shannon, 'Aberrations and their effects on images', SPIE Vol. 531: Geometrical Optics, Los Angeles, January 1985

[6] G.C. Holst, 'Electro-Optical Imaging System Performance', SPIE Optical Engineering Press, Winter Park, Florida 32789, p. 94, 2000

[7] A. Toet, J.W.A.M. Alferdinck, 'Effects of high power illuminators on vision through windscreens and driving behavior', SPIE Vol. 8898: Technologies for Optical Countermeasures X; and High-Power Lasers 2013: Technology and Systems, Dresden, September 2013

ACKNOWLEDGEMENT

This work was performed as a part of the Electronic Warfare Programme V1236, sponsored by the Netherlands MoD.